Pathogenic Role of PPARα Downregulation in Corneal Nerve Degeneration and Impaired Corneal Sensitivity in Diabetes

H. Greg Matlock,[1] Fangfang Qiu,[2] Volha Malechka,[3] Kelu Zhou,[1] Rui Cheng,[1] Siribhinya Benyajati,[1] Amy Whelchel,[1] Dimitrios Karamichos,[4,5] and Jian-xing Ma[1]

Diabetes 2020;69:1279–1291 | https://doi.org/10.2337/db19-0898

The purpose of this study was to investigate the protective role of peroxisome proliferator–activated receptor α (PPARα) against diabetic keratopathy and corneal neuropathy. Corneal samples were obtained from human donors with and without diabetes. Streptozotocin-induced diabetic rats and mice were orally treated with PPARα agonist fenofibrate. As shown by immunohistochemistry and Western blotting, PPARα was downregulated in the corneas of humans with diabetes and diabetic rats. Immunostaining of β-III tubulin demonstrated that corneal nerve fiber metrics were decreased significantly in diabetic rats and mice, which were partially prevented by fenofibrate treatment. As evaluated using a Cochet-Bonnet aesthesiometer, corneal sensitivity was significantly decreased in diabetic mice, which was prevented by fenofibrate. *PPARα*$^{-/-}$ mice displayed progressive decreases in the corneal nerve fiber density. Consistently, corneal sensitivity was decreased in *PPARα*$^{-/-}$ mice relative to wild-type mice by 21 months of age. Diabetic mice showed increased incidence of spontaneous corneal epithelial lesion, which was prevented by fenofibrate while exacerbated by *PPARα* knockout. Western blot analysis revealed significantly altered neurotrophic factor levels in diabetic rat corneas, which were partially restored by fenofibrate treatment. These results indicate that PPARα protects the corneal nerve from degeneration induced by diabetes, and PPARα agonists have therapeutic potential in the treatment of diabetic keratopathy.

Diabetic keratopathy, an ocular complication of diabetes, can manifest in a variety of forms, including persistent corneal epithelial defects, superficial punctate keratitis, corneal endothelial injury, and stromal opacification (1–3). In addition, established impacts of diabetes on the cornea include loss of corneal sensitivity, degeneration of nerve fibers (4), and corneal lesions. Approximately one out of four patients with diabetic keratopathy suffers from forms of keratoepitheliopathy, such as persistent corneal epithelial defects or recurrent corneal erosions (5). Although neurotrophic keratopathy is a rare, late complication of diabetes (6), recent studies indicate that corneal neurodegeneration occurs in the early stages of diabetes (4). Thus, keratoepitheliopathy may be a comparatively less severe complication caused by loss of normal trophic action of corneal nerve fibers (7).

In terms of potential new treatments for diabetic keratopathy, the well-known degeneration of corneal nerve fibers and loss of corneal sensitivity frequently associated with diabetes (8) have inspired considerable research on neurotrophic factors associated with functions such as neuronal differentiation and survival, neuritogenesis, synaptogenesis, and myelination. Clinical trials showed that nerve growth factor (NGF), glial cell–derived neurotrophic factor (GDNF), and other neurotrophic factors displayed potential benefits in the treatment of diabetic keratopathy and are considered promising (9). According to a study in mice, NGF and GDNF were reduced in the diabetic corneal epithelium with wounds compared with normal corneal epithelium, and neutralizing antibodies against NGF and GDNF impaired corneal nerve regeneration and neurite outgrowth from trigeminal ganglia

[1]Department of Physiology, The University of Oklahoma Health Sciences Center, Oklahoma City, OK
[2]Department of Ophthalmology, Tufts Medical Center, Boston, MA
[3]National Eye Institute, National Institutes of Health, Bethesda, MD
[4]Department of Ophthalmology, Dean McGee Eye Institute, The University of Oklahoma Health Sciences Center, Oklahoma City, OK
[5]Department of Cell Biology, The University of Oklahoma Health Sciences Center, Oklahoma City, OK

Corresponding author: Jian-xing Ma, jian-xing-ma@ouhsc.edu

Received 6 September 2019 and accepted 15 March 2020

This article contains supplementary material online at https://doi.org/10.2337/db20-4567/suppl.12000825.

(10). However, it remains to be elucidated which pathways can be therapeutically manipulated most effectively.

The association of peroxisome proliferator–activated receptor α (PPARα), a nuclear receptor activated by fatty acids, with regulation of neurotrophic factors has not been established in either the cornea or elsewhere. However, it has been speculated that the neurotrophic effects of oleic acid on neurons in the brain could be through PPARα activation (11). Also, ~500 articles have been published on the anti-inflammatory and neuroprotective properties of palmitoylethanolamide, a PPARα ligand (12). A link between PPARα and diabetic retinopathy became apparent after two prospective clinical trials, the Fenofibrate Intervention and Event Lowering in Diabetes (FIELD study) and the Action to Control Cardiovascular Risk in Diabetes (ACCORD) study. Both FIELD and ACCORD studies reported that fenofibrate, a PPARα agonist, was effective on diabetic retinopathy in patients with type 2 diabetes (13). Recent review articles have discussed PPARs, not only PPARα, as potential therapeutic targets in a wide variety of ocular diseases (14,15). Nonetheless, PPARα expression and function in the diabetic cornea has not been previously studied.

In summary, the etiology of diabetic keratopathy and corneal neuropathy are complex and only fragmentarily known; hence, effective treatments for these conditions remain lacking. PPARα expression levels in the diabetic cornea have not been measured. The aim of this study was to investigate a potential protective effect of fenofibrate against diabetic keratopathy and corneal neurodegeneration. We also addressed the hypothesis that PPARα confers a protective effect against the loss of nerve fibers in the aging and diabetic cornea by mechanisms that include stimulation of key neurotrophic pathways.

RESEARCH DESIGN AND METHODS

Ethics and Source of Human Corneal Samples

Corneal samples were obtained from human donors with type 1 and type 2 diabetes and control subjects without diabetes from the National Development and Research Institutes, Inc. and the Oklahoma Lions Eye Bank. All facets of the current study were in accord with the Declaration of Helsinki. The medical criteria for including donors with diabetes in this study can be found in Priyadarsini et al. (16).

Immunostaining of PPARα in Human Corneas

Human corneas were immunostained with 3,3′-diaminobenzidine as previously reported (17). The primary antibody was an anti-PPARα antibody (ab126285; Abcam, Cambridge, MA). The level of PPARα was quantified using ImageJ.

Animals

Male Sprague Dawley and Wistar rats were obtained from Charles River Laboratories (Wilmington, MA) at 8 weeks of age. C57BL/6J and *PPARα*$^{-/-}$ mice were from The Jackson Laboratory (Bar Harbor, ME). Diabetes was induced in rats with a single intraperitoneal injection of streptozotocin (STZ) (55 mg/kg body weight) at 2 months of age and in mice with five consecutive daily intraperitoneal injections of STZ (50 mg/kg body weight) at 3 months of age. Blood glucose measurements were made in fasted rats and mice using a OneTouch blood glucose meter (Johnson & Johnson/LifeScan, Chesterbrook, PA). Animals with fasting blood glucose levels >350 mg/dL were considered diabetic in this study. Animals were housed in a controlled environment facility with programmed 12-h light/dark cycle and fed ad libitum with water and standard laboratory rodent chow. The diabetic and nondiabetic treatment groups of rats were fed with chow containing 0.014% fenofibrate (5053; Purina) for 2 months in Sprague Dawley rats or for 4 months in Wistar rats, and C57BL/6J and *PPARα*$^{-/-}$ mice were fed fenofibrate chow for 6 months. We used two different diabetic periods in rats to observe the progression of the diabetic complications from early stages, when mechanistic changes can be detected, to latter stages, when effects can be observed. Care, use, and treatment of animals were according to The Association for Research in Vision and Ophthalmology's Statement for the Use of Animals in Ophthalmic and Vision Research. Experimental protocols were approved by The University of Oklahoma Health Sciences Center Institutional Animal Care and Use Committee. For imaging, animals were anesthetized via intraperitoneal injection with 50 mg/kg ketamine hydrochloride and 5 mg/kg xylazine (Vedco Inc., St. Joseph, MO), and pupils were dilated with topically administered 1% cyclopentolate solution (Wilson Ophthalmic, Mustang, OK) (Supplementary Fig. 1).

Corneal Sensitivity Measurements in Mice

In diabetic mice, corneal sensitivity was measured at 6, 7, and 8 months of age (3, 4, and 5 months after STZ injection). In C57BL/6J and *PPARα*$^{-/-}$ mice, corneal sensitivity was checked at 3-month intervals starting at 6 months of age (see Supplementary Fig. 1 for experimental flow chart). Corneal sensitivity was measured using a Cochet-Bonnet aesthesiometer (Luneau Technology, Pont-de-l'Arche, France) as previously described (18), except that a reading of 6.5 cm was recorded when the measurement at 6 cm caused an animal to become agitated.

Corneal Lesion Assessment in Mice

After each corneal sensitivity measurement, animals were inspected for corneal lesions, visually and with the aid of a MICRON III fundus camera (Phoenix Technology Group, Pleasanton, CA) and Olympus SZ40 stereomicroscope (Olympus Corporation, Waltham, MA). Lesions were graded according to established guidelines (19). For each inspection, a lesion was recorded for any lesion grade 1 or higher (e.g., from epithelial defects covering ~1% of the corneal area to epithelial and stromal defects covering a majority of the cornea area). Sample corneas were photographed with the fundus camera or a Nikon Coolpix S6150 digital camera.

Immunolabeling and Measuring Corneal Nerve Fiber Metrics in Mice and Rats

β-III tubulin immunolabeling of corneal nerve fibers was used to obtain fluorescent images to measure corneal nerve fiber density (CNFD) in rat and mouse corneal flat mounts with image quantification software discussed in the next paragraph. 3-Nitrotyrosine (3-NT) immunolabeling was used to quantify 3-NT in corneal sections of 12-month-old wild-type (WT) and *PPARα*$^{-/-}$ mice with diabetes. Animal cornea samples were dissected from rats and mice that had been euthanized by CO_2 gas asphyxiation (~5 min). The cornea samples were fixed and immunolabeled using a published protocol (18). The primary antibodies were an anti–β-III tubulin antibody (ab18207; Abcam) and an anti–3-NT antibody (ab61392; Abcam).

Corneal Nerve Fiber Metrics Analysis

With the aid of ACCMetrics software (University of Manchester), a clinical nerve fiber measurement program, images of fluorescent immunolabeled rat corneal nerve fibers (obtained as described above) were used to quantify nerve fiber density (20,21). For rats, five nonoverlapping areas with a field of view of 400 × 400 μm^2 in each corneal flat mount were randomly selected and photographed with a digital camera (Axioplan 2 imaging; Carl Zeiss, Jena, Germany). For mice, four 400 × 400-μm^2 nonoverlapping fields were selected from the central cornea, around the whorl, and not including the peripheral regions. ACCMetrics software detected approximately one-third of the visible subbasal plexus nerve fibers, and thus, the calculations were repeated after manually drawing over clearly visible subbasal plexus nerve fiber signals with Fiji software, similar to the semiautomated methods reported in the literature (22,23). ACCMetrics software detected subbasal plexus nerve fibers with negligible interference from stromal nerves. The average number per field was used to calculate CNFD for a given sample, and the sample averages were used to calculate CNFD. Each of the four fields was categorized according to the presence or absence of defects with an evidently cellular (nonartifactual) basis (e.g., loosely attached and/or enlarged cells and proteins aggregates/exudates). CNFD was calculated in all fields with defects and in all fields without defects for experimental and control mice.

Western Blot Analyses

Each cornea was dissected and lysed in radioimmunoprecipitation assay buffer for total protein analyses. To obtain the two fractions of interest, the epithelial and subbasal plexus nerve fibers were separated from the stromal layer by peeling away the softer tissues of the cornea with a rotary mortar. The remaining stromal layer was cut into fine pieces and homogenized. Primary antibody dilutions were 1:1,000 for the rabbit anti-PPARα antibody (ab126285; Abcam), 1:500 for a rabbit anti–brain-derived neurotrophic factor (anti-BDNF) antibody (ab108319; Abcam), 1:500 for a rabbit anti-GDNF antibody (ab64337; Abcam), and 1:5,000 for a mouse anti–β-actin antibody (A5441; Sigma-Aldrich, St. Louis, MO).

Statistical Analysis

Statistical analysis was performed using Prism 8 for Windows (GraphPad, San Diego, CA). Data were expressed as a percentage or mean ± SD. Quantitative data were analyzed using either unpaired Student *t* test for comparison between two groups at a time or one-way or two-way ANOVA for studies with more than two groups, followed by Bonferroni or Tukey multiple-comparisons test. $P < 0.05$ was considered statistically significant.

Data and Resource Availability

All data generated from this study are included in the manuscript. No applicable resources were generated or analyzed during the current study.

RESULTS

PPARα in Human Cornea in Diabetes

To determine if PPARα is expressed in the cornea and if its expression is altered in the corneas of humans with

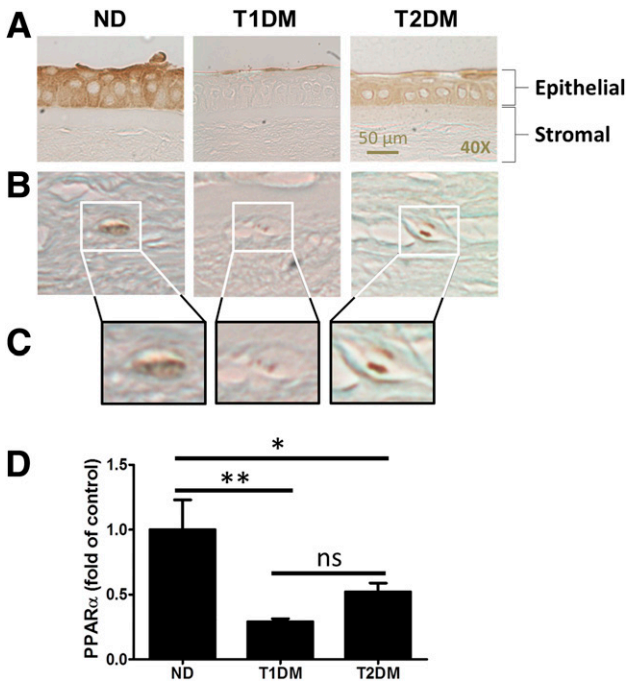

Figure 1—Human PPARα protein levels in the corneas from deceased patients with long-term diabetes (mean of 17 years). Representative images of immunostaining of corneal sections from three donors without diabetes (ND), three donors with type 1 diabetes mellitus (T1DM), and three donors with type 2 diabetes mellitus (T2DM) with an anti-PPARα antibody and stained with 3,3′-diaminobenzidine (brown). *A*: PPARα staining appeared weaker in the corneal epithelial cells in T1DM and T2DM than in ND. PPARα staining also appeared weaker in corneal epithelial cells of T1DM than in T2DM. *B*: Substantially lower PPARα staining was observed in the stromal layer in all groups. *C*: Enlarged images of the boxed areas in *B* showing decreased PPARα staining in T1DM and T2DM stromal cells. *D*: Quantification of PPARα IHC signal intensity (mean ± SD; $n = 3$). *$P < 0.05$; **$P < 0.01$.

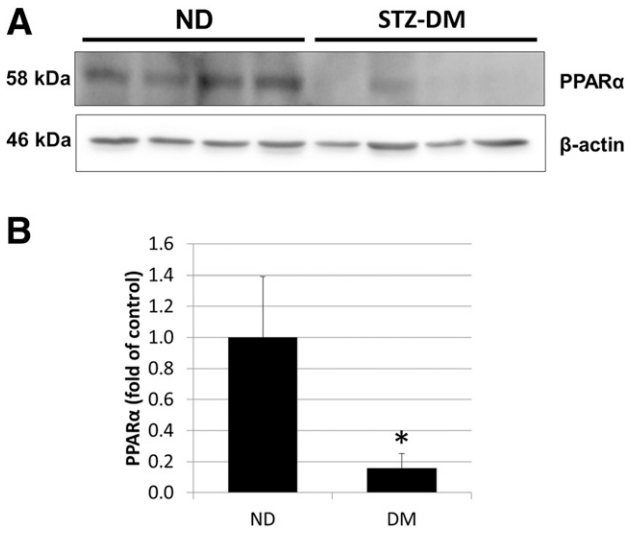

Figure 2—Protein levels of PPARα in whole cornea samples of diabetic and control rats. *A*: The protein level of PPARα was measured by Western blot analysis using an anti-PPARα antibody in the corneas of age-matched nondiabetic controls (ND) and rats with diabetes mellitus (STZ-DM) at 4 months after diabetes induction by STZ injection. *B*: PPARα protein levels were quantified by densitometry and normalized by β-actin levels (mean ± SD). $N = 4$. Blood glucose (mg/dL): ND, 96 ± 11; and STZ-DM, 458 ± 57. *$P < 0.01$.

diabetes, we used immunohistochemistry (IHC) with an antibody against PPARα on corneal sections from human donors with type 1 diabetes and type 2 diabetes and control subjects without diabetes. In nondiabetic corneas, intense PPARα signals were detected throughout the epithelial layer (Fig. 1*A*). Low expression of PPARα was detected in the stromal layer (Fig. 1*B* and *C*). Immunohistochemistry results demonstrated weaker PPARα immunosignals in the epithelial layer of corneal sections from donors with type 1 diabetes and type 2 diabetes compared with control subjects without diabetes (Fig. 1*D*). In the stromal layer, there were not enough cells to quantify PPARα, although it did appear qualitatively to be decreased in a similar pattern as the epithelium.

PPARα in the Cornea of Diabetic Rats

Next, we conducted Western blot analysis on STZ-injected diabetic rat cornea samples and nondiabetic rat controls to determine if corneal PPARα protein levels change in the diabetic rat model similar to those in humans with diabetes. The Western blot results showed that PPARα protein levels were significantly reduced in the corneas of diabetic rats with 4 months of STZ-induced diabetes compared with that in age- and genetic background–matched nondiabetic rats (Fig. 2).

Fenofibrate Ameliorated Loss of Corneal Nerve Fibers in Diabetic Rats

Diabetes is known to cause stromal edema (24) and increase the thickness and tortuosity of stromal nerves and subbasal nerves (25), and hence, it may reduce the density of stromal nerves (26) that support subbasal plexus nerves. To determine if PPARα deficiency in diabetic rats is related to the loss of corneal stromal nerve fibers, we measured CNFD in the stroma of diabetic rats with and without fenofibrate-supplemented diet and nondiabetic controls. Corneas from diabetic and nondiabetic rats were immunostained with an anti–β-III tubulin antibody, and nerve fiber metrics were quantified as described above. CNFD in diabetic rats was significantly decreased at 6 months of age (4 months of diabetes) (Fig. 3). Furthermore, fenofibrate treatment partially prevented the decrease in CNFD induced by diabetes (Fig. 3).

Decreased CNFD and Sensitivity in Diabetic Mice Were Partially Prevented by Fenofibrate

To determine if loss of corneal nerve fibers in diabetic mice results in decreases in corneal sensitivity, we compared CNFD and corneal sensitivity in diabetic mice and nondiabetic controls 3 months after the onset of diabetes. In addition, we measured corneal sensitivity at different time points after the onset of diabetes in diabetic mice and controls with and without fenofibrate treatment. We found that corneal sensitivity was significantly decreased at 5 months of diabetes in C57BL/6J mice (Fig. 4*A*). Fenofibrate treatment prevented the loss of corneal sensitivity at this time point. Consistently, diabetic mice showed decreased CNFD at 3 months of diabetes, which was partially restored by the treatment with fenofibrate (Fig. 4*B*).

Incidence of Corneal Lesions in Diabetic C57BL/6J Mice With Fenofibrate Treatment

To determine if activation of PPARα by fenofibrate protects against corneal lesions in diabetes, we treated C57BL/6J mice with STZ-induced diabetes with fenofibrate treatment for 5 months starting at 3 months of age. Nondiabetic WT mice had no apparent corneal lesions at 6, 7, and 8 months of age, while STZ-induced diabetic mice showed 8%, 9%, and 14% incidence of lesion, respectively (nonsignificantly higher than that in nondiabetic mice at the same ages). Fenofibrate-treated STZ-induced diabetic mice showed a nonsignificantly decreased incidence of corneal lesions, to the range of nondiabetic mice. In contrast, STZ-induced diabetic *PPARα*$^{-/-}$ mice had significantly increased incidence of corneal lesions in comparison with diabetic WT mice at 7 and 8 months of age (Fig. 4*C*).

PPARα Knockout Decreased Nerve Density in the Central Cornea

In order to investigate the role of PPARα in maintaining corneal nerve integrity, we quantified and compared CNFD in the corneas of *PPARα*$^{-/-}$ mice at 4, 7, 10, and 20 months of age and their age- and genetic background–matched WT mice. As shown by β-III tubulin staining, PPARα deficiency alone resulted in significantly decreased CNFD at 10 and 20 months (Fig. 5*A* and *C*). At 4 months of age, most

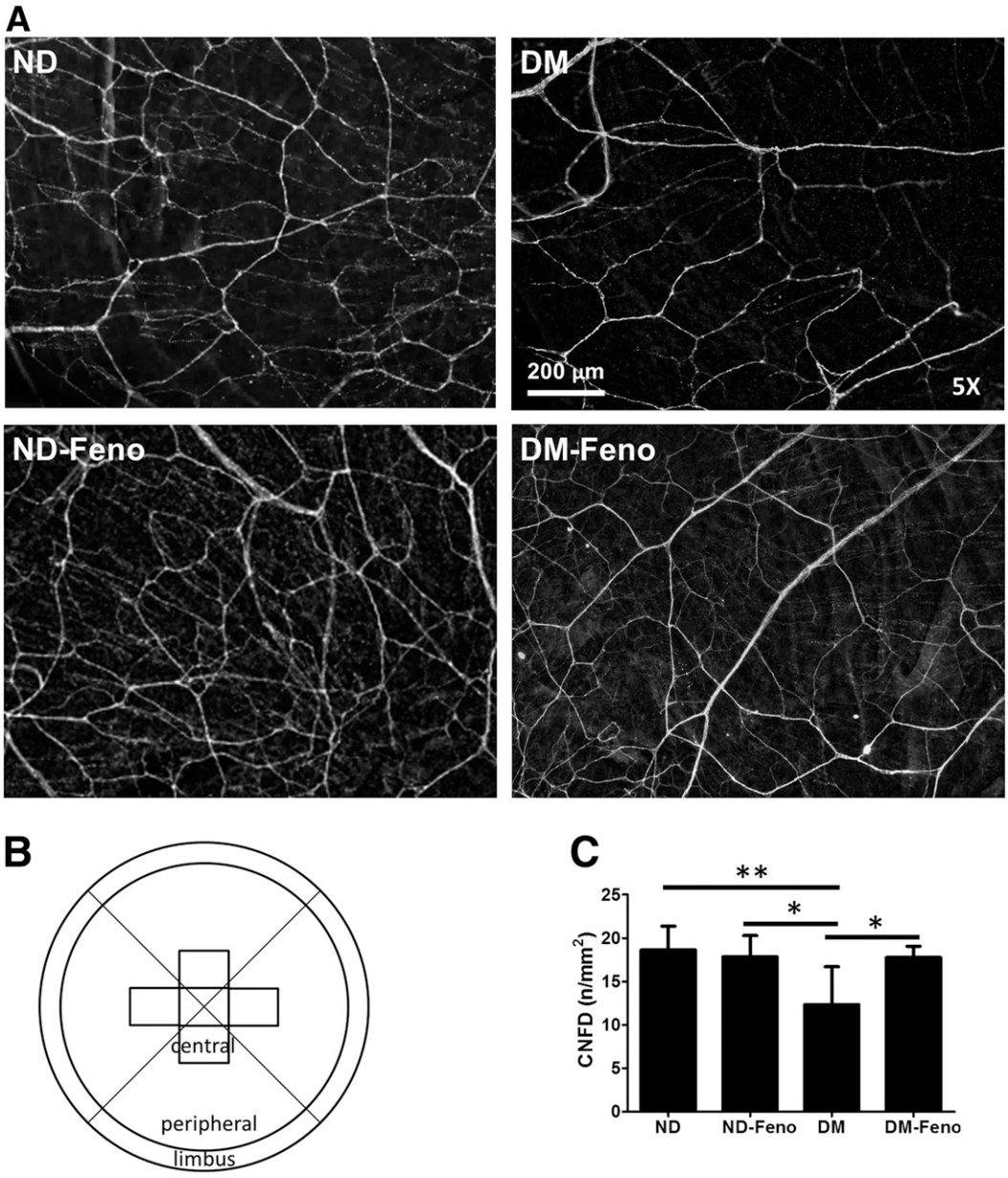

Figure 3—Effects of fenofibrate (Feno) treatment on corneal stromal nerve fibers in diabetic rats. Diabetes was induced with STZ injection at 2 months of age in Wistar rats. Rats with diabetes mellitus (DM) and age-matched nondiabetic rats (ND) were treated with chow containing 0.014% fenofibrate. *A*: At 6 months of age and after 4 months of diabetes, corneas from DM and ND rats as well as DM rats treated with fenofibrate (DM-Feno) and ND with fenofibrate (ND-Feno) were collected, immunolabeled with an anti–β-III tubulin antibody, flat-mounted, and viewed with a fluorescence microscope. *B*: Approximate location of corneal stromal nerve fiber images (3A) in the central cornea and around the vortex. *C*: CNFD was calculated using ACCMetrics software (University of Manchester). Mean ± SD. ND: $N = 9$; ND-Feno, $N = 4$; DM, $N = 6$; and DM-Feno, $N = 6$. Blood glucose (mg/dL): ND, 90 ± 9; ND-Feno, 99 ± 6; DM, 487 ± 53; and DM-Feno, 494 ± 61. *$P < 0.05$; **$P < 0.01$.

$PPAR\alpha^{-/-}$ mice lacked a vortex in the central corneal subbasal plexus; and, at all ages considered after 4 months, spacing of subbasal plexus nerve fibers was uneven in $PPAR\alpha^{-/-}$ mice compared with WT mice (Fig. 5*B*).

Progressive Decreases of Corneal Sensitivity in $PPAR\alpha^{-/-}$ Mice

Loss of nerve fibers can lead to decreased corneal sensitivity in aging and diabetes. To evaluate the impact of PPARα deficiency on age-related decline of corneal sensitivity, we measured corneal sensitivity in nondiabetic $PPAR\alpha^{-/-}$ mice and that in WT mice from 3 to 27 months of age at 3-month intervals. Corneal sensitivity showed more prominent decreases with age in $PPAR\alpha^{-/-}$ mice, reaching statistical significance at 21 months of age, compared with age- and genetic background–matched WT mice (Fig. 6).

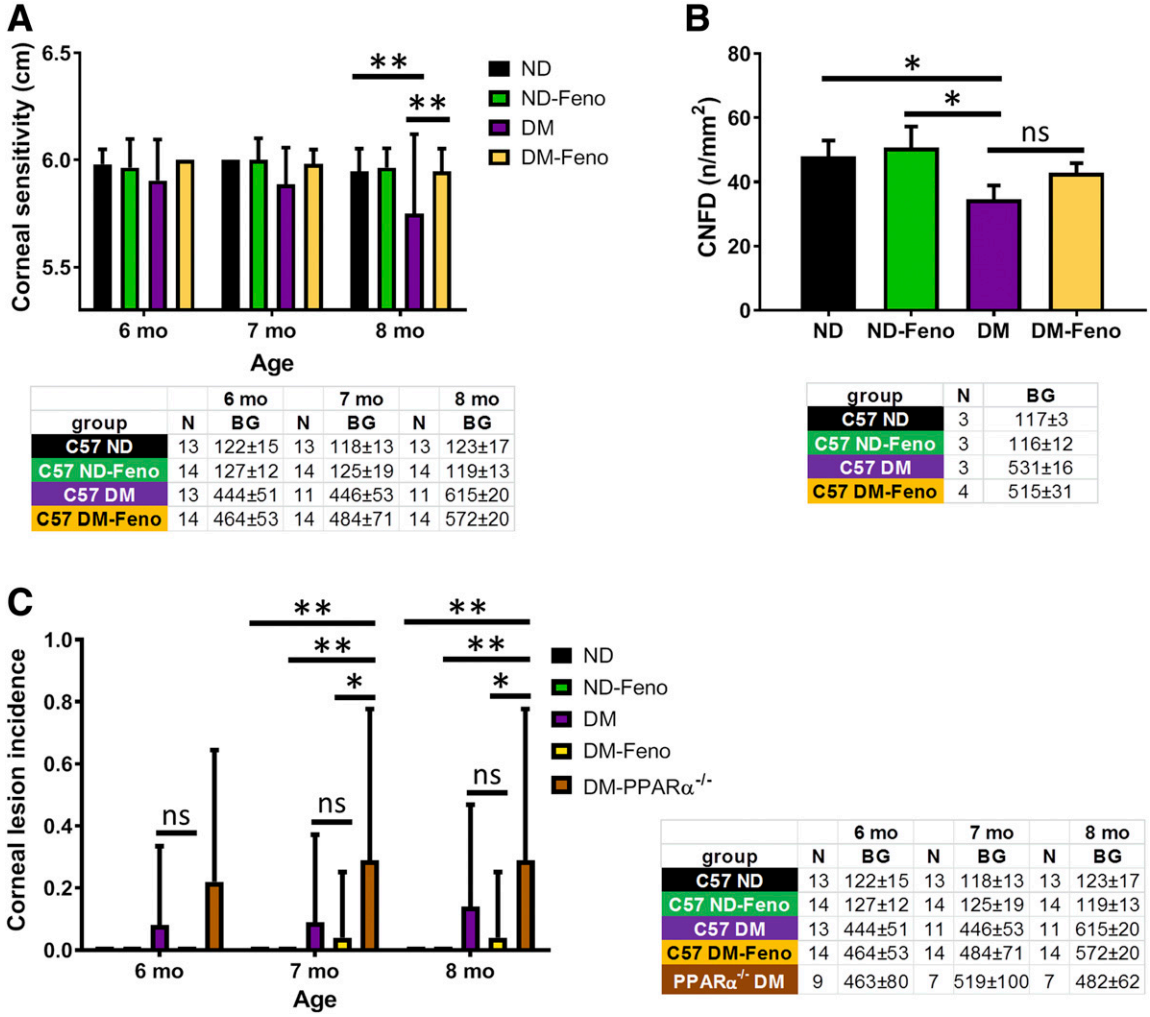

		6 mo		7 mo		8 mo
group	N	BG	N	BG	N	BG
C57 ND	13	122±15	13	118±13	13	123±17
C57 ND-Feno	14	127±12	14	125±19	14	119±13
C57 DM	13	444±51	11	446±53	11	615±20
C57 DM-Feno	14	464±53	14	484±71	14	572±20

group	N	BG
C57 ND	3	117±3
C57 ND-Feno	3	116±12
C57 DM	3	531±16
C57 DM-Feno	4	515±31

		6 mo		7 mo		8 mo
group	N	BG	N	BG	N	BG
C57 ND	13	122±15	13	118±13	13	123±17
C57 ND-Feno	14	127±12	14	125±19	14	119±13
C57 DM	13	444±51	11	446±53	11	615±20
C57 DM-Feno	14	464±53	14	484±71	14	572±20
PPARα-/- DM	9	463±80	7	519±100	7	482±62

Figure 4—Corneal sensitivity, lesions, and subbasal plexus nerve fiber density in STZ-diabetic mice. Diabetes was induced with STZ injections at 3 months of age in C57BL/6J mice. Both nondiabetic mice (ND) and mice with diabetes mellitus (DM) were fed with chow containing 0.014% fenofibrate (ND-Feno and DM-Feno). *A*: Corneal sensitivity in these mice was measured and compared in nondiabetic mice (ND) and mice with diabetes mellitus (DM) with regular chow at 6, 7, and 8 months of age (mean ± SD). $^{**}P < 0.001$. $N = 11–14$. *B*: CNFD of the subbasal plexus was measured using Fiji and ACCMetrics software (University of Manchester). Mean ± SD. $^{*}P < 0.05$. ND, $N = 3$; ND-Feno, $N = 3$; DM, $N = 3$; and DM-Feno, $N = 4$. *C*: Corneal lesion quantification in ND mice, DM mice with and without fenofibrate, and age-matched *PPARα*$^{-/-}$ mice with STZ-induced diabetes mellitus (DM-*PPARα*$^{-/-}$) (6-, 7-, and 8-month-old mice with 4 months of diabetes) (mean ± SD). $N = 7–14$. $^{*}P < 0.05$; $^{**}P < 0.001$. BG, blood glucose (mg/dL); mo, month.

Increased Incidence of Corneal Lesions in *PPARα*$^{-/-}$ Mice

In order to help establish the role of decreased central corneal nerve fibers in the development of corneal lesions, we compared corneal lesion incidence in *PPARα*$^{-/-}$ mice at 6, 9, 12, 15, 18, 21, 24, and 27 months of age with that in age-matched WT mice. Corneal lesions were observed in *PPARα*$^{-/-}$ mice, with the earliest indications of defects frequently observed in the epithelial layer between 15 and 18 months of age. In *PPARα*$^{-/-}$ mice, the incidence of corneal lesions of all types was noticeably higher at 15, 18, and 21 months of age and statistically significant at 21, 24, and 27 months of age in comparison with age-matched WT mice. The incidence of *PPARα*$^{-/-}$ mouse corneal lesions was significantly higher, beginning at 21 months of age in comparison with young *PPARα*$^{-/-}$ mice (Fig. 7*D*). No in vivo corneal lesions were apparent in *PPARα*$^{-/-}$ mice at 12 months of age, ∼2 months after CNFD reached statistical significance (Fig. 5*C*) and incidence of β-III tubulin IHC-visible epithelial lesions was at a minimum (Fig. 7*I*). Immunolabeling of 3-NT showed that the 3-NT signal was significantly increased in corneal sections of 12-month-old diabetic *PPARα*$^{-/-}$ mice, compared with that in diabetic WT mice (Fig. 7*C*).

Ex vivo experiments revealed a relationship between CNFD and β-III tubulin IHC-visible defects. Defects included irregular spacing of subbasal plexus nerve fibers,

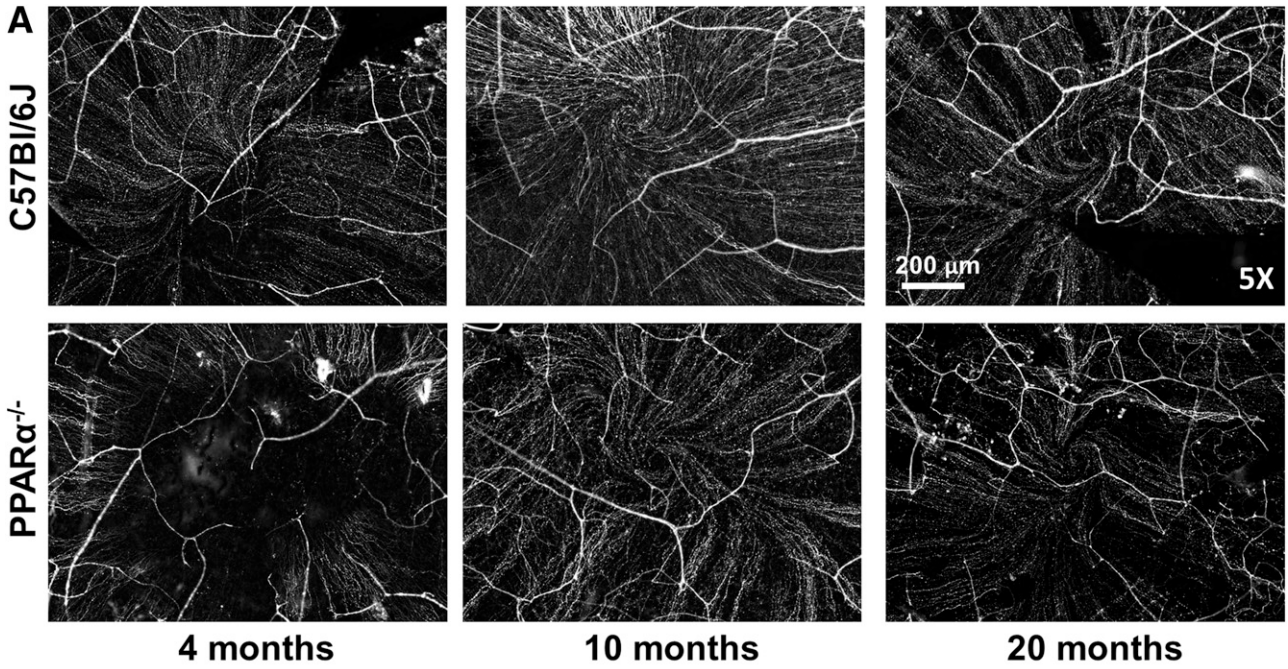

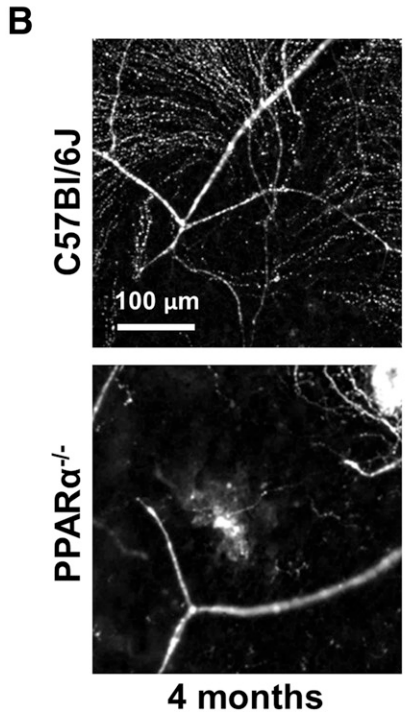

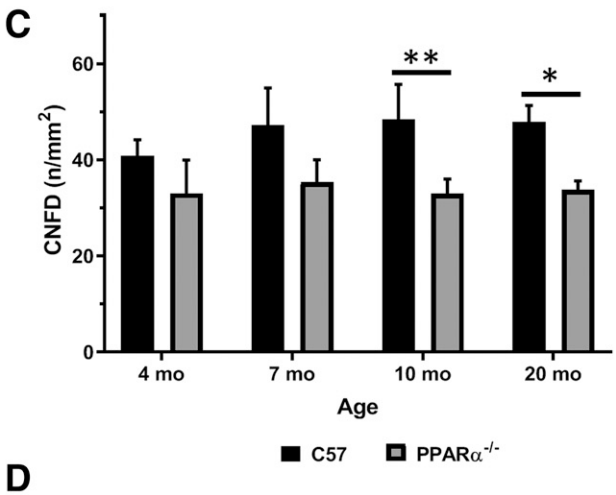

D

N	C57Bl/6J	w/out defect*	w/defect	PPARα$^{-/-}$	w/out defect*	w/defect
4 mo	6	4	2	13	5	8
7 mo	3	3	0	5	4	1
10 mo	9	8	1	4	2	2
20 mo	6	5	1	3	1	2
Total	24	20	4	25	12	13

Figure 5— Nerve fibers and nerve fiber–dependent defects in the cornea of *PPARα*$^{-/-}$ mice compared with WT mice from 4 to 20 months of age. Mice with no visible lesions or grade 1 lesions were included in this analysis. *A*: Representative images of mouse corneal nerve fibers immunolabeled with an antibody for β-III tubulin (as described before for rats) at the ages of 4, 10, and 20 months. *B*: Exploded view of the central cornea showing the late development of the subbasal plexus vortex pattern in *PPARα*$^{-/-}$ mice compared with WT C57BL/6J. *C*: Subbasal plexus CNFD for each cornea and age group was quantified using ACCMetrics software (University of Manchester). At 10 and 20 months of age, *PPARα*$^{-/-}$ mice had decreased CNFD compared with WT. Mean ± SD. *$P < 0.05$, **$P < 0.01$ vs. WT; for ages 4, 7, 10, and 20 months: WT, $N = 6, 3, 9$, and 6; and knockout, $N = 13, 5, 4$, and 3, respectively. *D*: Number of mice in each age group with (w/defect) and without (w/out defect) β-III tubulin IHC-visible corneal defects. mo, month.

β-III tubulin immunosignals in epithelial cells, and aggregates. Preulcerous epithelial β-III tubulin IHC-visible defects were detected in areas of sparse subbasal plexus nerve fibers in WT central cornea at 4 and 20 months of age and *PPARα*$^{-/-}$ central cornea at 4, 7, 10, and 20 months of age (Fig. 7*I*). At both 4 and 20 months of age, β-III tubulin IHC-visible epithelial lesion involved fewer cells in WT compared with multiple cells in *PPARα*$^{-/-}$ central cornea.

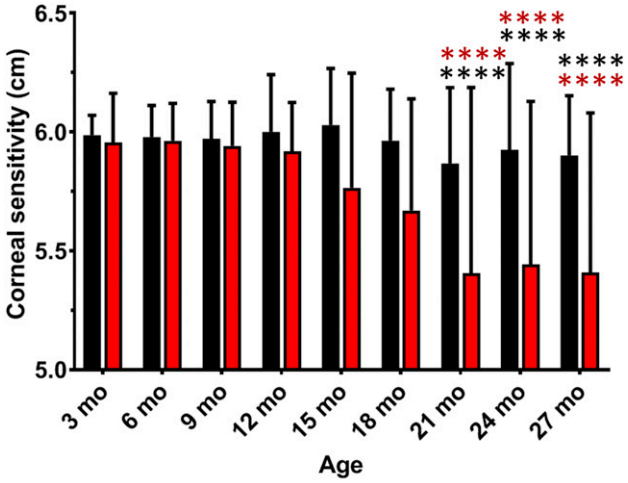

N value	6 mo	9 mo	12 mo	15 mo	18 mo	21 mo	24 mo	27 mo
N (C57Bl/6J)	35	35	35	35	34	34	34	33
N (PPARα$^{-/-}$)	34	34	34	34	34	34	33	30

Figure 6—Corneal sensitivity in *PPARα*$^{-/-}$ mice compared with WT C57BL/6J mice. Corneal sensitivity was measured using a Cochet-Bonnet aesthesiometer (Luneau Technology) in 0.5-cm filament steps from 6 cm (mean ± SD) at the indicated ages. Corneal sensitivity decreased significantly in *PPARα*$^{-/-}$ mice compared with C57BL/6J starting at 21 months of age. Mean ± SD. ****$P <$ 0.0001. mo, month.

For all ages combined (4, 7, 10, and 20 months), the incidence of IHC-visible lesion in *PPARα*$^{-/-}$ mice was significantly increased in comparison with WT mice ($P =$ 0.011). CNFD in fields with β-III tubulin IHC-visible corneal defects was compared with CNFD in fields without defects for *PPARα*$^{-/-}$ and WT mice in all age groups combined (4, 7, 10, and 20 months). IHC-visible corneal defects were significantly greater in areas with locally decreased nerve fiber for both *PPARα*$^{-/-}$ and WT mice (Fig. 7*J*).

Neurotrophic Pathways in Nondiabetic and Diabetic Cornea

To identify a mechanism underlying the role of diabetes-induced PPARα downregulation in corneal neuronal degeneration and lesions, we investigated the effects of diabetes and PPARα activation by fenofibrate on key neurotrophic factors in the corneas. We hypothesized that each neurotrophic factor could have different functions and levels of expression in *1*) the epithelial layer and subbasal plexus together, and *2*) the stromal layer and the stromal plexus. Considering that neurotrophic factors could be changed in different directions under diabetic conditions in each of these fractions, we separated corneal samples into two fractions: one containing the epithelial layer and subbasal plexus and the other containing the stromal layer and the stromal plexus for Western blot analysis.

As shown by Western blot analysis, GDNF (Fig. 8*A* and *B*) and BDNF (Fig. 8*C* and *D*) levels were altered in the diabetic rat corneas. GDNF levels were significantly decreased ($P = 0.019$) in the corneal epithelial and subbasal plexus fraction of diabetic rats (Fig. 8*A*). Dimeric BDNF (28 kDa) was decreased, although not significantly, in diabetic rat corneas in the corneal epithelial and subbasal plexus fraction relative to nondiabetic controls (Fig. 8*C*). Dimeric BDNF was not detected in the stromal fraction in either nondiabetic or diabetic rat corneas. Also, in the epithelial and subbasal plexus fraction, a cleavage fragment of proBDNF (24 kDa) (a possible activator of apoptosis) was significantly increased by ~160-fold in diabetic rat corneas relative to controls (Fig. 8*C*), whereas in the stromal fraction, proBDNF levels were drastically reduced (Fig. 8*D*).

PPARα was detected in the stromal fraction in diabetic corneas, although at low levels, and fenofibrate treatment had no significant effect here (Fig. 8*B*). Fenofibrate treatments significantly restored GDNF levels in the epithelial and subbasal plexus fraction in comparison with untreated diabetic cornea (Fig. 8*A*), but not significantly in the stromal fraction in diabetic rats (Fig. 8*B*). Fenofibrate treatment increased dimeric BDNF significantly in the corneal epithelial and subbasal plexus fraction (i.e., the nonstromal fraction) by 10-fold relative to diabetic rats with normal diet (Fig. 8*C*).

DISCUSSION

Effective treatments for diabetic corneal neuropathy and keratopathy are lacking, and the pathogenic mechanism underlying these conditions is uncertain. The current study demonstrated that PPARα levels are decreased in the cornea in both diabetic animal models and humans with diabetes. In addition, activation of PPARα partially ameliorated diabetes-induced corneal nerve degeneration and declined corneal sensitivity. PPARα knockout alone is sufficient to induce corneal nerve degeneration, impaired corneal sensitivity, and increased incidence of corneal lesions. The PPARα knockout animal is the first one that develops spontaneous characteristics seen in human diabetic keratopathy. These findings for the first time suggest that diabetes-induced PPARα downregulation plays an important pathogenic role in diabetic corneal complication and thus represents a novel therapeutic target.

PPARα is a transcription factor originally known to regulate lipid metabolism (27). Its expression and function in the diabetic cornea were not previously studied. Our studies demonstrated that PPARα is expressed in the corneas of the mouse, rat, and human, with high levels in the epithelium. Our data on human corneas indicate that, as in the pancreas (28) and the retina (29), PPARα is indeed downregulated in diabetic conditions (Fig. 1). Studies of diabetic rats demonstrated that PPARα is downregulated in diabetes in a similar manner as in humans (Fig. 2). Further, activation and upregulation of PPARα by fenofibrate protected against the damaging effects of diabetes on corneal nerve fiber functions and metrics. In rats, we observed significantly decreased CNFD because of diabetes, similar to reported effects of diabetes in humans. Also, in diabetic rats, oral treatment

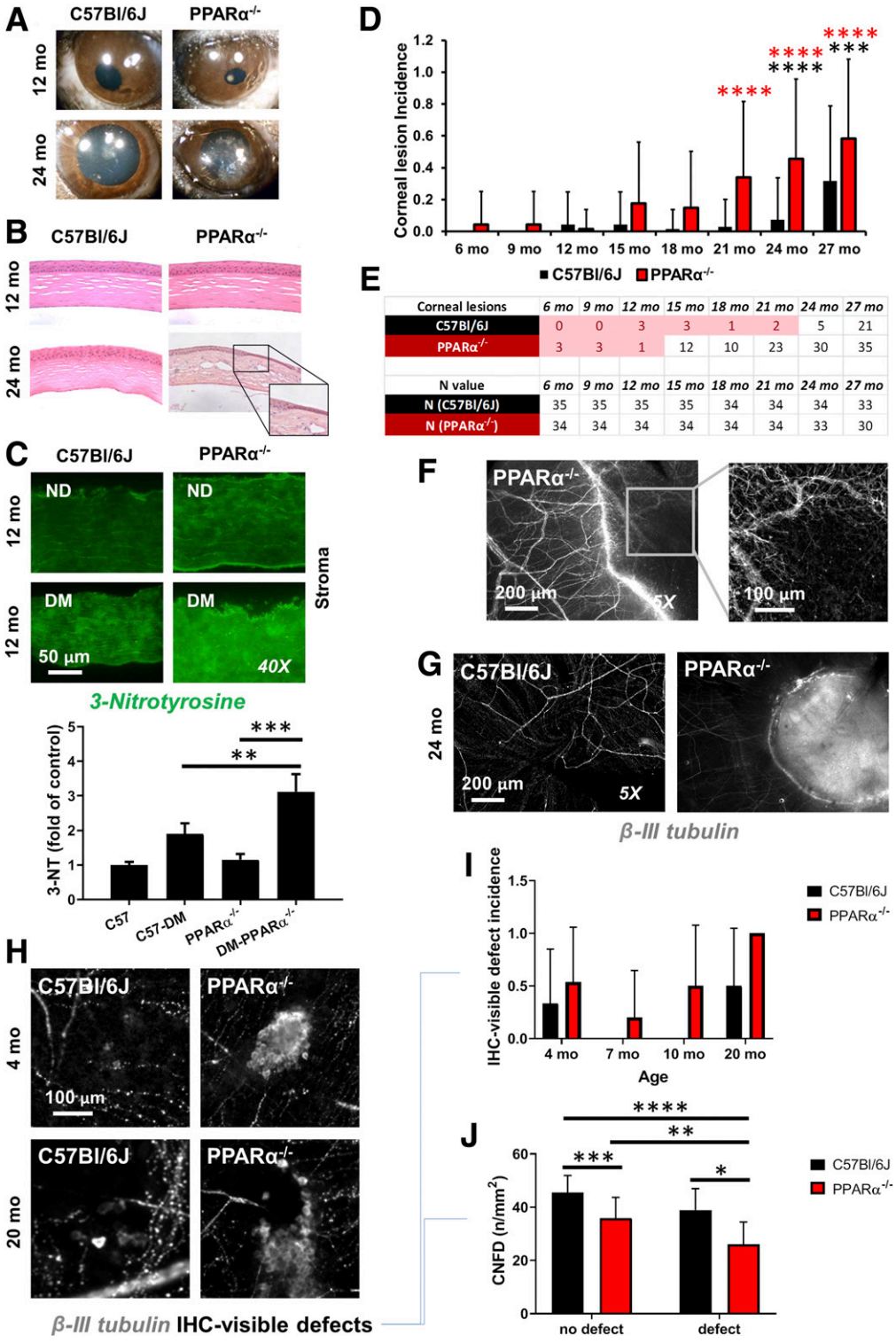

Figure 7—Cornea images, histology, corneal lesion incidence, and immunostaining of β-III tubulin and 3-NT in *PPARα*$^{-/-}$ and WT mice. *A*: Representative images of WT (C57BL/6J) and *PPARα*$^{-/-}$ mouse corneas with and without lesions photographed with a digital camera attached to a dissection microscope. *B*: At 12 months of age, hematoxylin and eosin staining confirmed frequent qualitative differences between *PPARα*$^{-/-}$ and WT corneas. *C*: Corneal sections of 12-month-old nondiabetic mice (ND), WT mice with diabetes mellitus (DM), and *PPARα*$^{-/-}$ mice immunolabeled with an anti–3-NT antibody showing increased 3-NT in WT and *PPARα*$^{-/-}$ mice with diabetes (mean ± SD). $^{**}P < 0.01$; $^{***}P < 0.001$. *D* and *E*: Incidence of corneal lesions in *PPARα*$^{-/-}$ and WT mice. Corneal lesions were observed from 6 to 27 months of age using a digital camera attached to a dissecting microscope. Corneal lesion incidence increased in *PPARα*$^{-/-}$ mice by 21 months of age compared with WT mice (mean ± SD; $^{***}P < 0.001$, $^{****}P < 0.0001$ relative to age-matched WT [black]; $^{****}P < 0.0001$ relative to young *PPARα*$^{-/-}$ [red]). *F*: Example of the effects of a severe lesion in a *PPARα*$^{-/-}$ cornea on nerve fiber immunostained using β-III tubulin antibody showing extremely dense and scrambled nerve fibers around and near the ulcer's border and in the deep stroma below the ulcer, and essentially no subbasal plexus nerve fibers more than ~50 μm inside the border of the ulcer. *G*: Flat-mounted whole corneas immunolabeled

with PPARα agonist fenofibrate partially prevented the decreases of CNFD caused by diabetes (Fig. 3). In the mouse cornea, STZ-induced diabetes had similar effects on corneal sensitivity, which is partly a function of nerve fiber density, as in humans with diabetes and diabetic rats (Fig. 4*A*). We found a decrease in corneal sensitivity in diabetic C57BL/6J mice, which was partially prevented by fenofibrate (Fig. 4*A*). These results suggest that activation of PPARα has protective effects against corneal nerve damage in diabetes.

To further investigate the role of PPARα in corneal nerve survival, we used *PPARα*$^{-/-}$ mice. Experiments on *PPARα*$^{-/-}$ mice revealed that PPARα deficiency alone resulted in decreased CNFD and corneal sensitivity, similar to that in diabetes in humans and rats, even though, as previous studies have already shown, *PPARα*$^{-/-}$ mice do not have high fasting blood glucose (30). In these mice, we observed decreased CNFD by 10 months of age (Fig. 5) and decreased corneal sensitivity by 21 months of age (Fig. 6). Together with the results of fenofibrate treatment, this finding suggests that PPARα is essential for maintaining the integrity of corneal nerves.

The lesion is another feature of diabetic corneal complication; however, the pathogenesis of corneal lesion is still obscure (6). Consistent with nerve fiber loss, our results showed that corneal lesion incidence is higher in diabetic mice compared with age-matched nondiabetic mice. Furthermore, fenofibrate treatment reduced incidence of corneal lesion in diabetic mice. In contrast, diabetic *PPARα*$^{-/-}$ mice displayed significantly higher incidence of corneal lesion compared with diabetic WT mice with the similar glucose levels and the same diabetes duration (Fig. 4*C*). Nondiabetic *PPARα*$^{-/-}$ mice had a significantly increased incidence of corneal lesions by 21 months of age compared with age-matched WT mice, which was the same age decreased corneal sensitivity was first observed (Fig. 7*D*) and 11 months after decreased CNFD and ex vivo β-III tubulin-visible lesions. β-III tubulin IHC-visible epithelial lesions were significantly higher in central cornea areas with locally decreased CNFD (Fig. 7*J*). These results suggest that diabetes-induced corneal lesion may be through, at least in part, downregulation of PPARα expression in the cornea.

Past studies of PPARα in other tissues have mainly addressed its regulatory roles in metabolic, inflammatory, and angiogenic pathways (31,32). Relatively few have addressed mechanisms involving neurotrophic factors. BDNF and GDNF are major neurotrophic factors that regulate neuronal and glial cell development and differentiation, functions, remodeling, and regeneration (33–36). In the cornea, it has been reported that BDNF plays a leading role in the process of nerve fiber repair and regeneration (37). GDNF promotes corneal epithelial cell proliferation (38). The current study investigated if PPARα protects corneal nerve under diabetic conditions through regulation of these neurotrophic factors in the cornea.

As shown by Western blot analysis, PPARα was present in both fractions of the cornea, the stromal fraction, and the epithelial and subbasal plexus fraction (Fig. 8). In STZ-induced diabetes, GDNF levels were significantly decreased in the epithelial and subbasal plexus fraction (Fig. 8*A*) and not significantly decreased in the stromal fraction (Fig. 8*B*). Fenofibrate treatment significantly increased PPARα and GDNF levels compared with those of untreated diabetic rats (Fig. 8*A*).

BDNF is known to function as a 28-kDa dimer that is extremely stable at physiological concentrations (and even 8 mol/L solutions of urea) (39). Our results indicated that BDNF dimer (28 kDa) was decreased in diabetes and increased approximately fourfold by fenofibrate treatment in the diabetic epithelial and subbasal plexus fraction. A documented study reported that proBDNF undergoes degradation, generating a 24-kDa fragment (40). Levels of a truncated form of proBDNF (24 kDa) were dramatically altered in diabetic rat corneas after 2 months of diabetes and in opposite ways in the stromal and nonstromal fractions of the cornea.

The regulation of BDNF expression by PPARα has not been documented previously. BDNF promoter sites have been studied extensively since 1993 (41) and contain no consensus on PPAR response elements. It is likely that PPARα regulates BDNF expression or protein degradation indirectly through a signaling pathway. The molecular mechanism for the regulation of BDNF by PPARα remains to be studied.

Our results indicate that fenofibrate increases the level of dimeric BDNF relative to the truncated form of proBDNF, which fits the emerging theory of BDNF mode of operation in the central nervous system. The critical balance between different forms of BDNF is a possible pathological mechanism underlying multiple sclerosis (42), chemotherapy-associated cognitive impairment (43), and cognitive impairment associated with type

with an anti–β-III tubulin antibody: representative images from central cornea region of 24-month-old WT mice showing no apparent epithelial lesions and central cornea region of a 24-month-old *PPARα*$^{-/-}$ mouse showing a severe ulcer. *H*: Four 400 × 400-μm nonoverlapping fields were selected from the central cornea and enhanced in Fiji software. Each field image was categorized according to the presence or absence of defects with an evidently subbasal plexus and/or epithelial cellular basis (e.g., loosely attached cells, enlarged groups of cells, and proteins aggregates/exudates). *I*: Ratio of cornea samples with β-III tubulin IHC-visible defects to samples without β-III tubulin IHC-visible defects at 4, 7, 10, and 20 months of age. *J*: CNFD in fields with β-III tubulin IHC-visible corneal defects was compared with CNFD in fields without defects for *PPARα*$^{-/-}$ and WT mice in all age groups combined (4, 7, 10, and 20 months). Mean ± SD. WT, $N = 24$; and knockout, $N = 25$. *$P < 0.05$, **$P < 0.01$, ***$P < 0.001$, ****$P < 0.0001$ relative to WT. C57, C57BL/6J; mo, month.

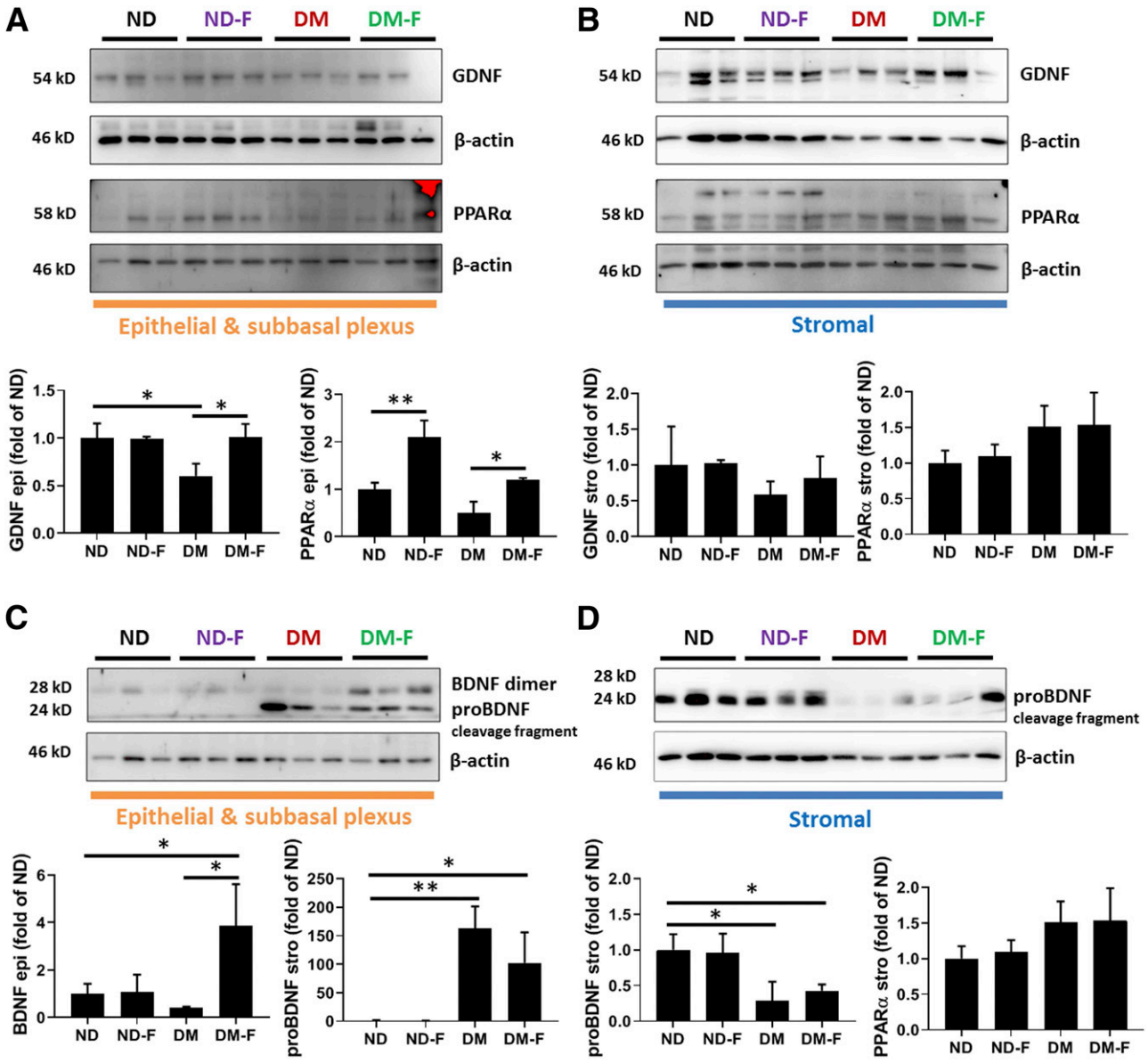

Figure 8—PPARα activation and neurotrophic factors in rat corneas. Neurotrophic factor proteins were measured in the corneas of nondiabetic (ND) rats, ND rats treated with fenofibrate (ND-F), rats with STZ-diabetes mellitus after 2 months of STZ injection (DM), and DM rats treated with fenofibrate (DM-F). *A*: In the epithelial and subbasal plexus fraction, GDNF oligomer (~54 kDa) was decreased but not significantly in DM rats compared with ND rats ($P = 0.062$; three ND and three DM rats). PPARα was significantly decreased by diabetes ($P = 0.031$; three ND and three DM rats). Fenofibrate diet significantly increased PPARα and GDNF ($P = 0.0301$ and $P = 0.04$, respectively). *B*: In the stromal fraction, GDNF (54 kDa) was not significantly different in the diabetic and fenofibrate-treated groups compared with controls. *C*: In the epithelial and subbasal plexus fraction, BDNF dimer (28 kDa) was significantly decreased in DM relative to ND, and fenofibrate significantly increased BDNF dimer. *D*: BDNF was not detected in the stromal fraction of either DM or ND corneas. The level of truncated proBDNF (24 kDa) was significantly decreased in all diabetic corneas compared with controls and not significantly increased in fenofibrate-treated diabetic corneas. Mean ± SD. $N = 3$. Blood glucose (mg/dL): ND, 111 ± 7; ND-Feno, 91 ± 14; DM, 563 ± 73; and DM-Feno, 581 ± 46. *$P < 0.05$; **$P < 0.001$. epi, epithelial; stro, stromal.

2 diabetes (44). This followed from the discovery that the proforms and truncated proforms of BDNF and other proneurotrophins activate the p75 neurotrophin receptor ($p75^{NTR}$), which modulates apoptotic signaling pathways and can trigger neuronal cell death when Trk receptors are absent (45), yet can also promote neuronal survival and neurite outgrowth when Trk receptors are present (46).

Summary

PPARα levels were decreased in corneas from humans with type 1 and type 2 diabetes and in diabetic rat corneas compared with nondiabetic rats. PPARα agonist fenofibrate protected corneal nerve fibers from degeneration and alleviated decreased corneal sensitivity in diabetic rats and diabetic mice. PPARα knockout in mice had effects similar

to diabetes on CNFD and corneal sensitivity. Also, diabetic *PPARα*$^{-/-}$ mice had higher incidences of corneal lesions than diabetic WT controls. BDNF and GDNF appear to play roles in mediating the neuroprotective effect of PPARα in diabetes. The results of our study revealed that fenofibrate could be an effective treatment for patients with diabetic keratopathy.

Acknowledgments. Shrestha Priyadarsini (Dean McGee Eye Institute, Oklahoma City, OK) prepared the human cornea samples used for immunolabeling. The authors thank the Diabetic Animal Core and Histology Core facilities of Diabetes CoBRE for the support of and assistance in this study.

Funding. This study was supported by National Eye Institute grants (EY018659, EY019309, EY012231, EY028949, and GM122744), JDRF grant (2-SRA-2019-711-S-B), and an Oklahoma Center for the Advancement of Science and Technology grant (HR16-041).

Duality of Interest. No potential conflicts of interest relevant to this article were reported.

Author Contributions. H.G.M., D.K., and J.-x.M. designed the experiments. H.G.M. conducted the experiments, researched data, and drafted the manuscript. H.G.M., F.Q., V.M., K.Z., R.C., and A.W. assisted with dissections and final grading of corneal lesions. S.B., D.K., and J.-x.M. reviewed and edited the manuscript. All authors approved the final version of the manuscript. J.-x.M. is the guarantor of this work and, as such, has full access to all of the data in the study and takes responsibility for the integrity of the data and the accuracy of the data analysis.

References

1. Herse PR. A review of manifestations of diabetes mellitus in the anterior eye and cornea. Am J Optom Physiol Opt 1988;65:224–230
2. Owen CG, Newsom RS, Rudnicka AR, Ellis TJ, Woodward EG. Vascular response of the bulbar conjunctiva to diabetes and elevated blood pressure. Ophthalmology 2005;112:1801–1808
3. Schultz RO, Matsuda M, Yee RW, Edelhauser HF, Schultz KJ. Corneal endothelial changes in type I and type II diabetes mellitus. Am J Ophthalmol 1984;98:401–410
4. Tavakoli M, Kallinikos PA, Efron N, Boulton AJ, Malik RA. Corneal sensitivity is reduced and relates to the severity of neuropathy in patients with diabetes. Diabetes Care 2007;30:1895–1897
5. Inoue K, Kato S, Ohara C, Numaga J, Amano S, Oshika T. Ocular and systemic factors relevant to diabetic keratoepitheliopathy. Cornea 2001;20:798–801
6. Lockwood A, Hope-Ross M, Chell P. Neurotrophic keratopathy and diabetes mellitus. Eye (Lond) 2006;20:837–839
7. Kowtharapu BS, Stahnke T, Wree A, Guthoff RF, Stachs O. Corneal epithelial and neuronal interactions: role in wound healing. Exp Eye Res 2014;125:53–61
8. Lambiase A, Bonini S, Micera A, Rama P, Bonini S, Aloe L. Expression of nerve growth factor receptors on the ocular surface in healthy subjects and during manifestation of inflammatory diseases. Invest Ophthalmol Vis Sci 1998;39:1272–1275
9. Wirostko B, Rafii M, Sullivan DA, Morelli J, Ding J. Novel therapy to treat corneal epithelial defects: a hypothesis with growth hormone. Ocul Surf 2015;13:204–212.e1
10. Di G, Qi X, Zhao X, Zhang S, Danielson P, Zhou Q. Corneal epithelium-derived neurotrophic factors promote nerve regeneration. Invest Ophthalmol Vis Sci 2017;58:4695–4702
11. Bento-Abreu A, Tabernero A, Medina JM. Peroxisome proliferator-activated receptor-alpha is required for the neurotrophic effect of oleic acid in neurons. J Neurochem 2007;103:871–881
12. Keppel Hesselink JM, Costagliola C, Fakhry J, Kopsky DJ. Palmitoylethanolamide, a natural retinoprotectant: its putative relevance for the treatment of glaucoma and diabetic retinopathy. J Ophthalmol 2015;2015:430596
13. Keech AC, Mitchell P, Summanen PA, et al.; FIELD Study Investigators. Effect of fenofibrate on the need for laser treatment for diabetic retinopathy (FIELD study): a randomised controlled trial. Lancet 2007;370:1687–1697
14. Khatol P, Saraf S, Jain A. Peroxisome proliferated activated receptors (PPARs): opportunities and challenges for ocular therapy. Crit Rev Ther Drug Carrier Syst 2018;35:65–97
15. Katome T, Namekata K, Mitamura Y, et al. Expression of intraocular peroxisome proliferator-activated receptor gamma in patients with proliferative diabetic retinopathy. J Diabetes Complications 2015;29:275–281
16. Priyadarsini S, Sarker-Nag A, Rowsey TG, Ma JX, Karamichos D. Establishment of a 3D in vitro model to accelerate the development of human therapies against corneal diabetes. PLoS One 2016;11:e0168845
17. Dorà NJ, Collinson JM, Hill RE, West JD. Hemizygous Le-Cre transgenic mice have severe eye abnormalities on some genetic backgrounds in the absence of LoxP sites. PLoS One 2014;9:e109193
18. Chucair-Elliott AJ, Zheng M, Carr DJ. Degeneration and regeneration of corneal nerves in response to HSV-1 infection. Invest Ophthalmol Vis Sci 2015;56:1097–1107
19. Harrison SM. Grading corneal ulcers. Ann Ophthalmol 1975;7:537–539, 541–542
20. Dabbah MA, Graham J, Petropoulos I, Tavakoli M, Malik RA. Dual-model automatic detection of nerve-fibres in corneal confocal microscopy images. Med Image Comput Comput Assist Interv 2010;13:300–307
21. Dabbah MA, Graham J, Petropoulos IN, Tavakoli M, Malik RA. Automatic analysis of diabetic peripheral neuropathy using multi-scale quantitative morphology of nerve fibres in corneal confocal microscopy imaging. Med Image Anal 2011;15:738–747
22. Byun YS, Kang B, Yoo YS, Joo CK. Poly(ADP-Ribose) polymerase inhibition improves corneal epithelial innervation and wound healing in diabetic rats. Invest Ophthalmol Vis Sci 2015;56:1948–1955
23. Holmes TJ, Pellegrini M, Miller C, et al. Automated software analysis of corneal micrographs for peripheral neuropathy. Invest Ophthalmol Vis Sci 2010;51:4480–4491
24. Gül M, Emre S, Eşrefoğlu M, Vard N. Protective effects of melatonin and aminoguanidine on the cornea in streptozotocin-induced diabetic rats. Cornea 2008;27:795–801
25. Mocan MC, Durukan I, Irkec M, Orhan M. Morphologic alterations of both the stromal and subbasal nerves in the corneas of patients with diabetes. Cornea 2006;25:769–773
26. Frueh BE, Körner U, Böhnke M. Confocal microscopy of the cornea in patients with diabetes. Klin Monatsbl Augenheilkd 1995;206:317–319 [in German]
27. Gervois P, Torra IP, Fruchart JC, Staels B. Regulation of lipid and lipoprotein metabolism by PPAR activators. Clin Chem Lab Med 2000;38:3–11
28. Roduit R, Morin J, Massé F, et al. Glucose down-regulates the expression of the peroxisome proliferator-activated receptor-alpha gene in the pancreatic beta -cell. J Biol Chem 2000;275:35799–35806
29. Hu Y, Chen Y, Ding L, et al. Pathogenic role of diabetes-induced PPAR-α down-regulation in microvascular dysfunction. Proc Natl Acad Sci U S A 2013;110:15401–15406
30. Guerre-Millo M, Rouault C, Poulain P, et al. PPAR-alpha-null mice are protected from high-fat diet-induced insulin resistance. Diabetes 2001;50:2809–2814
31. Devchand PR, Keller H, Peters JM, Vazquez M, Gonzalez FJ, Wahli W. The PPARalpha-leukotriene B4 pathway to inflammation control. Nature 1996;384:39–43
32. Panigrahy D, Kaipainen A, Huang S, et al. PPARalpha agonist fenofibrate suppresses tumor growth through direct and indirect angiogenesis inhibition. Proc Natl Acad Sci U S A 2008;105:985–990

33. Gaudet AD, Popovich PG, Ramer MS. Wallerian degeneration: gaining perspective on inflammatory events after peripheral nerve injury. J Neuroinflammation 2011;8:110
34. Heumann R, Lindholm D, Bandtlow C, et al. Differential regulation of mRNA encoding nerve growth factor and its receptor in rat sciatic nerve during development, degeneration, and regeneration: role of macrophages. Proc Natl Acad Sci U S A 1987;84:8735–8739
35. Binder DK, Scharfman HE. Brain-derived neurotrophic factor. Growth Factors 2004;22:123–131
36. Zhou Q, Chen P, Di G, et al. Ciliary neurotrophic factor promotes the activation of corneal epithelial stem/progenitor cells and accelerates corneal epithelial wound healing. Stem Cells 2015;33:1566–1576
37. Chaudhary S, Namavari A, Yco L, et al. Neurotrophins and nerve regeneration-associated genes are expressed in the cornea after lamellar flap surgery. Cornea 2012;31:1460–1467
38. You L, Kruse FE, Völcker HE. Neurotrophic factors in the human cornea. Invest Ophthalmol Vis Sci 2000;41:692–702
39. Radziejewski C, Robinson RC, DiStefano PS, Taylor JW. Dimeric structure and conformational stability of brain-derived neurotrophic factor and neurotrophin-3. Biochemistry 1992;31:4431–4436
40. Mandel AL, Ozdener H, Utermohlen V. Identification of pro- and mature brain-derived neurotrophic factor in human saliva. Arch Oral Biol 2009;54:689–695
41. Timmusk T, Palm K, Metsis M, et al. Multiple promoters direct tissue-specific expression of the rat BDNF gene. Neuron 1993;10:475–489
42. Tongiorgi E, Sartori A, Baj G, et al. Altered serum content of brain-derived neurotrophic factor isoforms in multiple sclerosis. J Neurol Sci 2012;320:161–165
43. Ng T, Lee YY, Chae JW, et al. Evaluation of plasma brain-derived neurotrophic factor levels and self-perceived cognitive impairment post-chemotherapy: a longitudinal study. BMC Cancer 2017;17:867
44. Zhen YF, Liu XY, Zhou DH, et al. Cognition, serum BDNF levels, and BDNF Val66Met polymorphism in type 2 diabetes patients and healthy controls. Oncotarget 2017;9:3653–3662
45. Salehi AH, Roux PP, Kubu CJ, et al. NRAGE, a novel MAGE protein, interacts with the p75 neurotrophin receptor and facilitates nerve growth factor-dependent apoptosis. Neuron 2000;27:279–288
46. DeFreitas MF, McQuillen PS, Shatz CJ. A novel p75NTR signaling pathway promotes survival, not death, of immunopurified neocortical subplate neurons. J Neurosci 2001;21:5121–5129